Studies of Light Neutron-Excess Nuclei from Bounds to Continuum

Makoto Ito

Department of Pure and Applied Physics, Kansai University, Suita 565-0821, Japan

The generalized two-center cluster model (GTCM), which can handle various single particle configurations in general two center systems, is applied to the light neutron-rich system, $^{12}\mathrm{Be} = \alpha + \alpha + 4N$. We discuss the change of the neutrons' configuration around two α-cores as a variation of an excitation energy. The covalent, ionic and atomic configurations coexist with the degenerate feature above the $\alpha + {}^{8}\mathrm{He}_{g.s.}$ particle-decay threshold. We find the strong enhancement in the monopole excitation from the ground state to the excited states. The GTCM calculation is also applied to even Be isotopes, and the systematics on the structural changes from bound region to continuum is discussed.

§1. Introduction

In the last two decades, developments of experiments with secondary RI beam have extensively advanced the studies on light neutron-rich nuclei. In particular, much efforts have been devoted to the investigation of molecular structure in Be isotopes. The Be isotopes can be considered as typical examples of two-center superdeformed systems which build on an $\alpha + \alpha$ rotor of ^{8}Be. Theoretically, molecular orbital (MO), such as the π^- and σ^+ orbitals associated with the covalent bonding in atomic molecules, have been successful in understanding the low-lying states of these isotopes.[1)]

The MO model can describe many kinds of characteristic properties of these isotopes, but they are mainly limited to the analysis on low-lying bound states, and theoretical studies on the highly excited states above the particle-decay threshold is still open area. In contrast to the situation of theoretical studies, recent experiments on ^{12}Be, for instance, revealed the existence of many resonant states,[2)–4)] which strongly decay into $^{6}\mathrm{He}_{g.s.} + {}^{6}\mathrm{He}_{g.s.}$ and $\alpha + {}^{8}\mathrm{He}_{g.s.}$. Similar resonances, decaying to He isotopes, have also been observed in other Be isotopes, such as $^{10}\mathrm{Be} = \alpha + {}^{6}\mathrm{He}$ and $^{14}\mathrm{Be} = {}^{6}\mathrm{He} + {}^{8}\mathrm{He}$.

In the present study, we investigate the structural changes from the bound states to the continuum states in even Be isotopes. In order to investigate the continuum states above the particle decay threshold, the intrinsic structures and their coupling to the scattering states should be treated in a unified manner. For this purpose, we introduce the generalized two-center cluster model (GTCM).[5)] In this model, the covalent MO configuration can be smoothly connected to the atomic or ionic one, in which valence neutrons are localized around one of the α cores. Furthermore, it becomes possible to describe both the formation of the covalent MO structures and its decays into a continuum energy state.[6)] In this report, we mainly investigate the intrinsic structure of ^{12}Be and enhancement phenomena in the monopole transitions of $0^+_{g.s.} \to 0^+_{ex.}$, which is embedded in continuum. We also apply GTCM to even

Be isotope of $^{8\sim16}$Be, and investigate the structural changes from a bound region to continuum region.

§2. Framework

The detailed explanation of GTCM has already been published in Refs. 5) and 6), and we briefly show the formulation of GTCM in the following. In this model, the total wave function of ^{12}Be is given by the superposition of the basis $\{\Phi_{\boldsymbol{m}}^{J^\pi K}(S)\}$, where,

$$\Phi_{\boldsymbol{m}}^{J^\pi K}(S) = \hat{P}_K^{J^\pi} \mathcal{A} \left\{ \psi_L(\alpha)\psi_R(\alpha) \prod_{j=1}^{4} \varphi_j(m_j) \right\}_S \quad . \tag{2·1}$$

The α-cluster $\psi_n(\alpha)$ $(n = L, R)$ is expressed by the $(0\mathrm{s})^4$ configuration of the harmonic oscillator (HO) centered at the left(L)- or right(R)- side with the relative distance S. The single-particle wave function for the four valence neutrons localized around one of the α clusters is given by an atomic orbital (AO) $\varphi(p_k, i, \tau)$, and $0p$-orbitals p_k $(k = x,\ y,\ z)$ around i $(= L$ or $R)$ with the spin τ $(= \uparrow$ or $\downarrow)$. Here, $\{m_j\}$ are indices of AO (p_k, i, τ) and $\boldsymbol{m}$ represents a set of AOs for the four neutrons, $\boldsymbol{m} = (m_1, m_2, m_3, m_4)$. The intrinsic basis functions with the full anti-symmetrization $\mathcal{A}$ are projected to the eigenstate of the total spin J, its intrinsic angular projection K, and the total parity π by the projection operator $\hat{P}_K^{J^\pi}$.

The total wave function is finally given by taking the superposition over S, $\boldsymbol{m}$ and K as

$$\hat{\Psi}_\nu^{J^\pi} = \int dS \sum_{\boldsymbol{m},K} C_{\boldsymbol{m}K}^{\nu}(S)\, \Phi_{\boldsymbol{m}}^{J^\pi K}(S) \quad . \tag{2·2}$$

The coefficients for the ν-th eigenstate, $C_{\boldsymbol{m}K}^{\nu}(S)$, are determined by solving a coupled channel GCM (Generator Coordinate Method) equation.[8] We include all the possible AO configurations for the four valence neutrons within the axially symmetric $(K = 0)$ case.[5)–7)] As for the nucleon-nucleon interaction, we use the Volkov No. 2 and the G3RS for the central and spin-orbit parts, respectively. The parameters in the interactions and the size parameter of HO are the same as those applied in Refs. 5)–7), which successfully reproduce the properties of ^{10,12}Be.

§3. Results

3.1. *Energy levels in ^{12}Be*

The application of GTCM to $^{12}\mathrm{Be} = \alpha + \alpha + 4N$ has already been published in Ref. 6). In ^{12}Be, various chemical-bonding-like states, such as the covalent MO states (0_1^+ and 0_2^+), the ionic states of $\alpha + {}^8\mathrm{He}_{g.s.}$ and ${}^5\mathrm{He}_{g.s.} + {}^7\mathrm{He}_{g.s.}$($0_3^+$ and 0_6^+), the atomic state of ${}^6\mathrm{He}_{g.s.} + {}^6\mathrm{He}_{g.s.}$($0_4^+$), and the covalent-atomic hybrid state of $({}^5\mathrm{He} + {}^5\mathrm{He})(\sigma_{1/2}^{+})^2(0_5^+)$, appear.[7]

The comparison of the resonant levels ($0_3^+ \sim 0_6^+$) with the respective He-decay thresholds are summarized in Fig. 1. In this figure, the six-body channels, α + α + $4N$ is also plotted although the degree of freedom for the six-body decay is not considered in the present calculation. Since the calculated threshold difference, $\Delta E = E_{th}(^6\mathrm{He}_{g.s.} + {}^6\mathrm{He}_{g.s.}) - E_{th}(\alpha + {}^8\mathrm{He}_{g.s.})$, is larger by about 1.3 MeV than the experimental value, the thresholds and the energy levels above $E_{th}(^6\mathrm{He}_{g.s.} + {}^6\mathrm{He}_{g.s.})$ are shifted by 1.3 MeV to the lower energy side. One to one correspondence between the levels and the thresholds is also clearly confirmed in other levels. The cluster structures change from level to level according to the threshold rules.

As shown in Fig. 1, all the threshold energies are confined within the range of $\sim$ 4 MeV, and the energy interval is just $\sim$1 MeV. Because of the small energy spacings, the mixing of the He-cluster components is strong. The dominant populations in the individual levels are about 50% in average. Such a mixture among the channels is important for reducing the decay width of the levels.[7]

The level scheme of the unbound states nicely reproduce the features in the recent observation, obtained in the inelastic scattering of ^{12}Be by an α target.[4] In this inelastic scattering, the 0^+ strength, which reveals the overlapping resonant behavior with the interval of $\sim$ 1 MeV, is observed in the same energy region as the present calculation. Furthermore, at least, there are two observed levels consistent to the calculated levels;[7] the calculated 0_3^+ and 0_5^+ states have a dominant decay width into the $\alpha + {}^8\mathrm{He}_{g.s.}$ and $^6\mathrm{He}_{g.s.} + {}^6\mathrm{He}_{g.s.}$ channels, respectively, and two levels having the similar decay schemes are observed around the same energy regions.

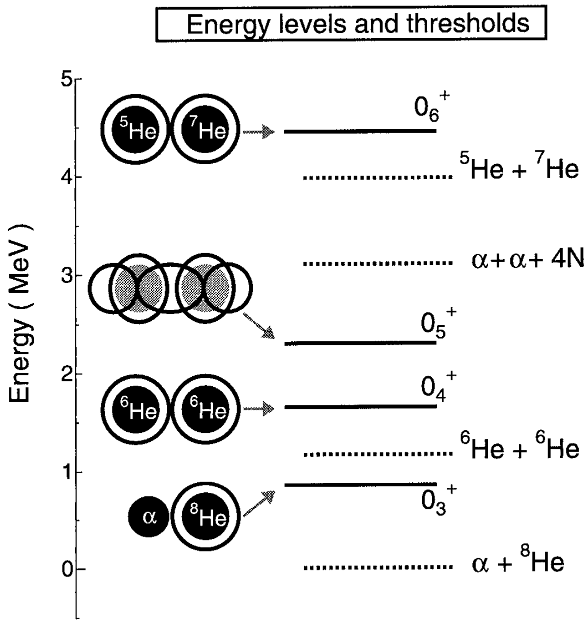

Fig. 1. Energy levels in the continuum. The threshold for the binary He channels (calculation) and the α + α + $4N$ (experiment) are shown by the dotted lines, while the energy levels are plotted by the solid lines. The threshold and the energy levels above $E = 1$ MeV are shifted by about 1.3 MeV. See text for details.

3.2. *Monopole transitions in ^{12}Be*

All the excited states have a large magnitude of the (isoscalar) monopole transition from the ground ($\nu = 1$) state to the ν-th 0^+ states,[9] which is defined by

$$M(IS) = \langle \Psi^\nu | \sum_{i=1}^{12} r_i^2 \mid \Psi^1 \rangle \equiv \langle 0_\nu^+ | \sum_{i=1}^{12} r_i^2 \mid 0_1^+ \rangle \ . \qquad (3\cdot1)$$

Here r_i denotes the radial coordinate for the i-th nucleon in ^{12}Be. In general neutron-excess systems, an isovector part of monopole matrix elements does not vanish and

Table I. The ratio of the total monopole strength and the single particle strength in the $0p$-shell.

State	Main configuration	Ratio
0_2^+	$(\pi_{3/2}^-)^2(\pi_{1/2}^-)^2$	2.59
0_3^+	$\alpha + {}^8\mathrm{He}_{g.s.}$	3.53
0_4^+	${}^6\mathrm{He}_{g.s.} + {}^6\mathrm{He}_{g.s.}$	0.92
0_5^+	$({}^5\mathrm{He} + {}^5\mathrm{He})(\sigma_{1/2}^+)^2$	1.48
0_6^+	${}^5\mathrm{He}_{g.s.} + {}^7\mathrm{He}_{g.s.}$	1.76

contributes to the total strength of a monopole transition. However, the isovector excitation becomes zero if the target nucleus is an isospin-saturated system, such as the α particle. In recent experiments, nuclear reactions with an α target are often employed to probe excited states of neutron excess systems.[4] In this study, therefore, we consider only the isoscalar part of the monopole matrix element.

In order to discuss the magnitude of the monopole strength clearly, in Table I, we show the ratio of the calculated strength to the respective single particle strength, $|M(IS)/M^{s.p.}|$.[10] All the strength is comparable to or a few times larger than the single particle strength, $M^{s.p.}$, and these values are almost the same magnitude as the transition to the 0_2^+ state at $E_x = 7.65$ MeV in ^{12}C, having a 3α cluster structure. In ^{12}C, the ratio of the monopole strength of $0_1^+ \to 0_2^+$ is about 4.6.[11] The result of ^{12}Be is consistent to the analysis of the monopole strength in Ref. 10), where the enhancement of the low-lying monopole strength is discussed by cluster formations. It should be noted that all the monopole strength, corresponding to the various cluster structures, appears at $E_x \leq 20$ MeV in the present system. In marked contrast to this result, in a naive mean-field picture, a $2\hbar\omega$ (~ 35 MeV) jump is needed for monopole excitations. This means that it is quite difficult to explain the monopole strength shown in Table I by mean-field models and hence, the present result is considered to be abnormal in a naive single particle picture.

In a system with a considerable neutron excess, there are almost degenerate monopole states at much lower energies than the energy region expected in a naive shell-model picture, and the transition strengths to these states are comparable with the single-particle strength. Among the various 0^+ states, strong enhancement occurs for the transition to the 0_3^+ state ($\alpha + {}^8\mathrm{He}_{g.s.}$), which is generated by an excitation of the α-α relative motion from the ground state. An enhancement can also be seen for the 0_2^+ state with the two neutrons' excited configuration, $(\pi_{3/2}^-)^2(\pi_{1/2}^-)^2$. This enhancement is due to the mixing of $(\pi_{3/2}^-)^2(\sigma_{1/2}^+)^2$ and $(\pi_{3/2}^-)^2(\pi_{1/2}^-)^2$ as pointed out in Ref. 12). However, the strength for 0_3^+ is about two times the magnitude of the strength for 0_2^+, and the transition to the cluster excited state, 0_3^+, is strongest in all the monopole strength.

3.3. *Systematics of even Be isotopes*

We discuss the systematics of even Be isotopes by applying the similar GTCM calculation. The energy spectra of ^{10}Be with $J^\pi = 0^+$ is shown in Fig. 2(a). The

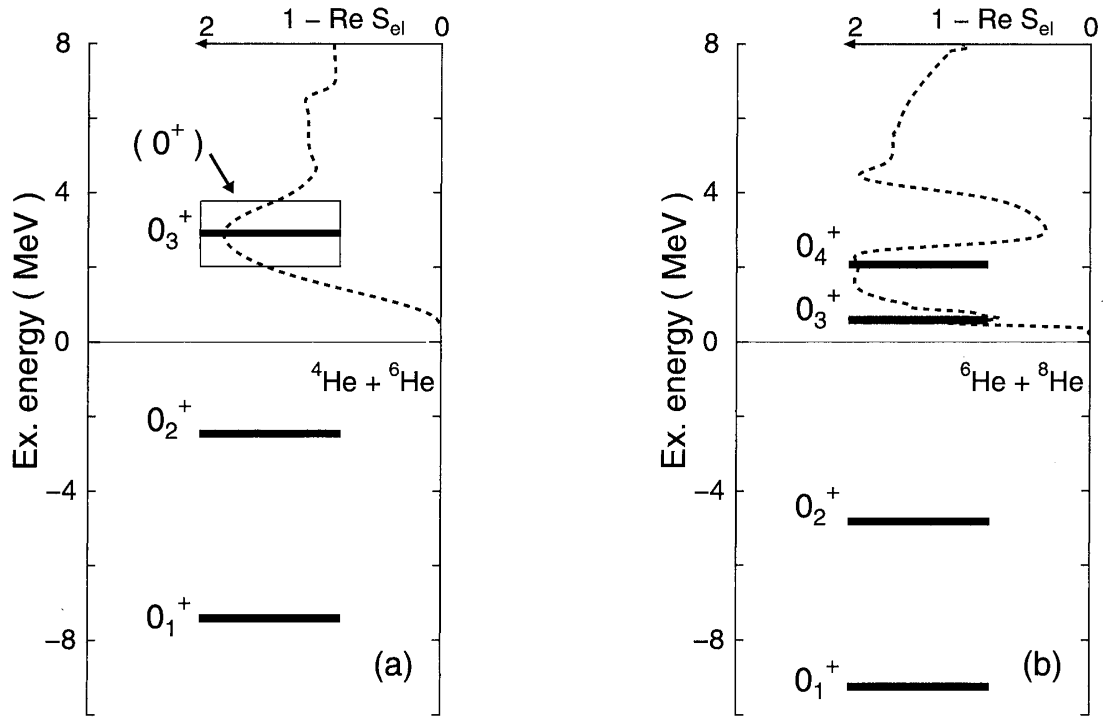

Fig. 2. (a) Energy spectra of ^{10}Be ($J^{\pi} = 0^{+}$). The threshold energies of the $\alpha + {}^{6}\mathrm{He}_{g.s.}$ channel is taken to be the origin. The dotted curve at the right part represents the reaction probability for the central collision of $\alpha + {}^{6}\mathrm{He}_{g.s.}$. (b) The same figure as (a) but for ^{14}Be. The ${}^{6}\mathrm{He}_{g.s.} + {}^{8}\mathrm{He}_{g.s.}$ threshold energy is set to be the origin.

total reaction probability, $1 - \Re S_{el}$, which is defined by the scattering matrices of the $\alpha + {}^{6}\mathrm{He}_{g.s.}$ elastic scattering (S_{el}), is plotted by the dotted curve at the upper part in Fig. 2(a).

Below the α decay threshold (zero energy point), two bound states appear. The intrinsic structures of the 0_1^+ and 0_2^+ states are nicely described by the MO configuration of $(\pi_{3/2}^-)^2$ and $(\sigma_{1/2}^+)^2$, respectively. Since the $\sigma_{1/2}^+$ orbit has an enlarged distribution along the α-α axis, the α-α clustering is well developed in the 0_2^+ state. Above the α decay threshold, the ionic states are realized as continuum resonant states. A prominent peak appears around $E \sim 3$ MeV in the total reaction probability. This enhancement of the reaction probability is due to the formation of the resonance with the ionic structure of $\alpha + {}^{6}\mathrm{He}(2_1^+)$, which is shown by the 0_3^+ state in Fig. 2(a). At the same energy region, there is a broad continuum strength, shown by 0^+ in parenthesis with a transparent box. This continuum state has a main component of an ionic structure of $\alpha + {}^{6}\mathrm{He}_{g.s.}$. Two 0^+ states embedded in continuum correspond to the higher nodal state from the bound states, which are formed by the nodal excitation of the α-α relative wave function: The 0_3^+ state is the nodal excited states from the ground 0_1^+ state, while the continuum (0^+) involves the similar α-α nodal excitation from the 0_2^+ state.

The energy spectra for ^{14}Be is shown in Fig. 2(b). In this figure, we can clearly confirm the similar level structure to ^{10}Be. In the bound region, two 0^+ states appears, while two resonant states are embedded in continuum energy. The ground 0_1^+ state has a spatially compact structure, which can be nicely understood by the shell model picture, while the 0_2^+ state has a well developed α-α cluster structure. Furthermore, two resonant states are identified by solving the $^6\mathrm{He} + {}^8\mathrm{He}$ collision, and they have the ionic structures, such as $^6\mathrm{He}_{g.s.} + {}^8\mathrm{He}_{g.s.}(0_3^+)$ and $^6\mathrm{He}(2_1^+) + {}^8\mathrm{He}_{g.s.}(0_4^+)$. The 0_3^+ and 0_4^+ states correspond to the two α's relative excitation from the two bound states, the 0_1^+ and 0_2^+ states, respectively.

We have also analyzed the level structure of $^{16}\mathrm{Be}$. There is a possibility of the resonance formation of a nuclear dimer such as $^8\mathrm{He}_{g.s.} + {}^8\mathrm{He}_{g.s.}$ although $^{16}\mathrm{Be}$ itself is an unstable nucleus with respect to two neutrons emission. The ratio of N/A in the $^8\mathrm{He}$ nucleus is 0.75, which is the highest value in bound nuclear systems. Thus, the $^8\mathrm{He}+{}^8\mathrm{He}$ atomic state corresponds to the nuclear dimers with extremely neutron excess, and it is very interesting to investigate the possibility of its formation. We have found that the ground state in $^{16}\mathrm{Be}$ appears below the $^8\mathrm{He}_{g.s.}+ {}^8\mathrm{He}_{g.s.}$ threshold by about 4 MeV. This ground state corresponds to the unbound states with respect to the $^{14}\mathrm{Be}_{g.s.} + 2n$ threshold by about 3 MeV. The ground state in $^{16}\mathrm{Be}$, which is predicted by the GTCM calculation, can be considered as an analog state of α+α in $^8\mathrm{Be}$. The analysis of the wave functions is in progress.

§4. Summary

We have studied the exotic structures of $^{12}\mathrm{Be}$ by applying GTCM. Above the α decay threshold, various chemical-bonding-like structures appear with the small energy interval. In the continuum energy region, one to one correspondence between the levels and the thresholds is clearly confirmed. The cluster structures with the neutrons' chemical bonds change from level to level according to the threshold rules.

All the energy levels have the monopole strength comparable to or larger than the single particle strength. In particular, the largest strength is predicted for the 0_3^+ state, which is generated by the α-α excitation from the ground state directly. These enhancements in the monopole transition can be observed in the much lower energy region than the energy region in the shell model expectation. Various excited states are obtained in even Be isotopes of $^{8\sim16}\mathrm{Be}$. The strong monopole enhancement can also be expected in the excited states of $^{10,14}\mathrm{Be}$. The systematic analysis on the monopole transition is now underway.

References

1) N. Itagaki and S. Okabe, Phys. Rev. C **61** (2000), 044306, and references therein.
2) A. A. Korsheninnikov et al., Phys. Lett. B **343** (1995), 53.
3) M. Freer et al., Phys. Rev. C **63** (2001), 034301.
4) A. Saito et al., Mod. Phys. Lett. A **25** (2010), 21.
5) M. Ito, K. Kato and K. Ikeda, Phys. Lett. B **588** (2004), 43.
M. Ito, N. Itagaki and K. Ikeda, Phys. Rev. C **85** (2012), 014302.
6) M. Ito and K. Yabana, Prog. Theor. Phys. **113** (2005), 1047.
M. Ito, Phys. Lett. B **636** (2006), 293.
7) M. Ito, N. Itagaki, H. Sakurai and K. Ikeda, Phys. Rev. Lett. **100** (2008), 182502.
M. Ito and N. Itagaki, Phys. Rev. C **78** (2008), 011602(R); Phys. Rev. Focus **22** (2008), Story 4.
M. Ito and D. Suzuki, Phys. Rev. C **84** (2011), 014608.

8) H. Horiuchi et al., Prog. Theor. Phys. Suppl. No. 62 (1977), 1.
9) M. Ito, Phys. Rev. C **83** (2011), 044319.
10) T. Yamada et al., Prog. Theor. Phys. **120** (2008), 1139.
11) M. Kamimura, Nucl. Phys. A **351** (1981), 456.
12) Shimoura et al., Phys. Lett. B **654** (2007), 87.